Combustion and Flame 160 (2013) 933–946

Contents lists available at SciVerse ScienceDirect

Combustion and Flame

journal homepage: www.elsevier.com/locate/combustflame

MILD oxy-combustion of gaseous fuels in a laboratory-scale furnace

Pengfei Li [a], Bassam B. Dally [b], Jianchun Mi [a,*], Feifei Wang [a]

[a] State Key Laboratory of Turbulence and Complex Systems, Department of Energy & Resources Engineering, College of Engineering, Peking University, Beijing, China
[b] Center of Energy Technology & School of Mechanical Engineering, The University of Adelaide, Australia

ARTICLE INFO

Article history:
Received 30 August 2012
Received in revised form 14 January 2013
Accepted 25 January 2013
Available online 20 February 2013

Keywords:
MILD combustion
Flameless oxidation
Oxy-combustion
O_2/CO_2 combustion

ABSTRACT

The present study investigates the characteristics of Moderate or Intense Low-oxygen Dilution (MILD) oxy-combustion in a laboratory-scale furnace. Experiments using natural gas (NG), liquefied petroleum gas (LPG) and ethylene (C_2H_4) are carried out at a firing rate of 13 kW. The furnace temperatures and exhaust emissions are measured for a range of equivalence ratios and external-CO_2 dilution rates.

It is observed that MILD combustions occur for the three fuels even when using pure oxygen as oxidant. When diluting oxidant by CO_2 at a fixed rate, the MILD combustion can be established as long as the equivalence ratio (Φ) is sufficiently high. The region of MILD combustion is found to be wider with dilution by CO_2 than by N_2. Notably, also, the operating range of MILD combustion is larger for NG than LPG or C_2H_4 as fuel.

Moreover, when $\Phi < 1$, as Φ is increased, the furnace temperature rises slightly but the NO_x emission decreases. This cannot be explained when using the traditional thermal NO_x mechanism. Indeed, using various NO mechanism models, our calculations show very low NO emissions resulting from the thermal, prompt and NNH routes but a much higher value from the N_2O-intermediate route. Namely, only the latter mechanism plays a crucial role in forming NO. Also important is that the NO reburning appears to reduce NO emissions notably and so should not be ignored in the MILD combustion.

1. Introduction

Oxy-combustion has generated significant interest for carbon capture and storage (CCS) [1–3]. This technology also has additional benefits such as emission reduction and lower costs of flue gas cleanup [4–6]. By eliminating nitrogen from the combustion medium, the flue gas will consist mainly of CO_2 and H_2O. Recirculated combustion products are used for diluting a nearly pure O_2 stream. Due to the higher heat capacity and radiative properties of CO_2 compared to N_2, an increased initial oxygen concentration (23–35%) for this combustion is required to achieve gas temperatures and heat transfer performances similar to those in air–fuel combustion [7,8]. The flue gas can then undergo a condensation process to remove H_2O to end up with a flue gas that consists almost entirely of CO_2. The nearly pure CO_2 product stream obtained via this process is suitable for use in enhanced oil recovery (EOR), coal bed methane (CBM) production, or geologic sequestration [9]. More recently, this technology has been adopted to substitute the original integrated gasification combined cycles (IGCC) plan in the US DOE FutureGen 2.0 program [10]. Details on the characteristics [4,6,11,12] and combustion process [4], as well as recent developments in plot-scale and commercial-scale demonstration plants [13] of the oxy-fuel combustion, can be found in the above mentioned articles.

While successful, the technology still faces many challenges [4]. At least three features of the oxy-fuel combustion process need to be better understood: (a) the approach of further increasing the thermal performance of the system, (b) the subsequent potential of NO_x forming, due to leakage of air (air-ingress) or nitrogen in the fuel itself [5], and (c) the challenge of improving the stabilization of oxy-fuel combustion due to the lower adiabatic flame temperature, delayed ignition and lower burning rate in a CO_2 diluted environment [4,14–16]. However, the increase of the flame temperature and combustion intensity, which is one of the approaches for further increasing the thermal performance, often comes at the price of high pollutant emissions (e.g., NO_x) [17]. Although NO_x emissions can be controlled by air or fuel staging, or low-NO_x burner technology, the flame temperature is also decreased undesirably. It is difficult to simultaneously satisfy the requirements of high efficiency and low pollution in oxy-fuel combustion process. One way of addressing this is to use the principle of MILD combustion.

MILD combustion is an efficient and clean combustion technology [18–26]. Extremely low NO_x emission and simultaneously high thermal efficiency can be achieved in the MILD combustion process. To our best knowledge, the three groups, i.e., Wünning and Wünning [20], Nippon Furnace Kogyo Kaisha Ltd. (NFK-Japan)

* Corresponding author.
E-mail address: jcmi@coe.pku.edu.cn (J. Mi).

0010-2180/$ - see front matter © 2013 The Combustion Institute. Published by Elsevier Inc. All rights reserved.
http://dx.doi.org/10.1016/j.combustflame.2013.01.024

Nomenclature

Symbols

A_o	area of the nozzle exit (m^2)
c_p	volumetric heat capacity at constant pressure (kJ/(m^3 K))
D_{ex}	diameter of the exhaust outlet (mm)
D_f	diameter of the fuel nozzle exit (mm)
D_o	diameter of the oxidant nozzle exit (mm)
h	lower heating value of the fuel (kJ/kg)
J	jet momentum rate (kg m/s^2)
J_f	fuel jet momentum rate (kg m/s^2)
J_o	oxidant jet momentum rate (kg m/s^2)
K_v	relative recirculation rate
K_v^*	external relative dilution rate
M_d	total mass flow rate of diluents (kg/s)
M_e	mass flux of the external diluents (kg/s)
M_f	fuel jet mass flux (kg/s)
M_i	mass flux of internal entrained exhaust gas (kg/s)
M_o	oxidant jet mass flux (kg/s)
m_o	jet mass flux (kg/s)
P	thermal input power rate (kW)
T	furnace temperature (K)
T_p	preheat temperature of oxidant
T_{ad}	adiabatic flame temperature (K)
T_{max}	maximum temperature (K)
T_w	furnace wall temperature (K)
U_o	velocity of the initial reactant
Y^f_{CO2}	initial mass fraction of CO_2 in the fuel jet (%)
Y^o_{CO2}	initial mass fraction of CO_2 in the oxidant jet (%)
Y^o_{O2}	initial mass fraction of O_2 in the oxidant jet (%)

Greek letters

λ	thermal conductivity (W/(m K))
α	mass diffusivity in air (m^2/s)
υ	kinematic viscosity (m^2/s)
ρ_o	density of the initial reactant (kg/m^3)
Φ	equivalence ratio

[19,21] and the International Flame Research Foundation (IFRF) [22,23], have originally been involved in the development of this technology. In the German path [20,24], from the early 1990s, this technology was named as flameless oxidation (FLOX). In the period from 1992 to 1999, the NFK-Japan and the IFRF worked together and the Japan-IFRF design [19] was distinct from the design of Wünning and Wünning [20]. The IFRF reports, e.g., [25], in the period from 1992 to 1999 and the journal publications, e.g., Weber et al. [23], described the experimental and numerical results. Later, Cavaliere and Joannon et al. [18,26] introduced the acronym MILD for the technology, which has been well recognized by the international combustion community.

The main advantages of MILD combustion are uniform temperature distribution, increased net radiation flux, extremely low NO_x emissions and the stable operating of the combustion mode without flame stabilization problem [20,27–33]. Theoretically, if the oxy-fuel technology is combined with the MILD technology to achieve the MILD oxy-fuel combustion, the thermal efficiency may be improved and simultaneously the NO_x emission may be suppressed. Hence, the MILD oxy-combustion may have the potential to offer more advantages over the standard oxy-combustion [4].

Although a good volume of work has been carried out in the separate field of the MILD combustion [28–33] and the oxy-fuel combustion, the information on the combination of the MILD combustion and oxy-fuel combustion is limited. The IFRF tested MILD oxy-NG combustion in a project called OXY-FLAM [34,35] in the period from 1995 to 1999, although without CO_2 recirculation. The project dealt both with the detailed characterization of oxy-combustion burners and with the validation of new computer codes as sub-models for oxy-NG combustion calculations. The experimental work included input–output and measurements in flames in the thermal input range 0.7–1.0 MW. They found good predictions by using the eddy dissipation concept mode with the full equilibrium chemistry procedure [34,35]. Blasiak et al. [36] applied the oxy-NG combustion to thermal treatment processes of wastes and the recovery of zinc bearing feed on a rotary kiln. They found that the MILD oxy-combustion not only increases the productivity of the rotary kiln but also reduces the fuel consumption and NO_x emissions. Krishnamurthy et al. [37] compared conventional and MILD oxy-combustion under similar conditions using propane as fuel (200 kW). They found that the MILD oxy-combustion can be achieved by asymmetric injection of high velocity oxygen (at near sonic velocities). They also found that the soot formation was negligible in MILD and was higher in conventional flame mode. Krishnamurthy et al. [38] also found that the NO_x emission of MILD oxy-combustion can be maintained at very low levels and is insensitive to air-ingress. The air leakage was indicated by the amount of oxygen in the flue gases. For conventional flame combustion, the NO_x emission increases as oxygen level of the exhaust increases. Their test was performed in a pilot-scale furnace (8 m^3) where air-ingress into the combustion chamber was simulated by leaking air into it, in order to raise the free oxygen content in the combustion gases. The oxygen content was measured in the furnace flue gas outlet. Stadler et al. [39] developed a high speed injection MILD oxy-combustion 100 kW burner. Their experimental setup has successfully achieved stable MILD oxy-combustion with 15% oxygen volume concentration as compared to 17% with a standard swirl burner. Stadler et al. [40] also found that the flue gas recirculation led to a reduction of NO_x emissions of up to 50% for the swirl flame, whereas in MILD combustion this reduction is around 40% compared to CO_2/O_2. Heil et al. [41] presented an experimental investigation of methane MILD oxy-combustion with different inert gases (N_2/O_2 and CO_2/O_2) and O_2 concentrations (21 vol% and 18 vol%). The result demonstrated that by eliminating the influences of molar heat capacity, CO_2 dissociation and thermal radiation, the effects of high CO_2 concentrations on combustion rates can be attributed to its participation in the chemical reactions. An increase of O_2 led to a reduction of this impact. Despite the above investigations, the basic information on the MILD oxy-combustion is still sparse and calls for more research.

To help address the above deficit, the present study is designated to investigate the detailed performance and stability characteristics of a parallel jet burner system operating at a laboratory-scale MILD combustion furnace burning NG, LPG and C_2H_4 with air or O_2/CO_2 mixture. This is achieved through the measurements of in-furnace temperatures, exhaust emissions and stability limits. The NO_x formation mechanisms are investigated from the computational fluid dynamic (CFD) simulation. Effects of the initial mass fraction of CO_2, equivalence ratio, burner configuration, fuel type, and thermal field are also discussed. Finally, the stability limits of MILD oxy-combustion at different oxidant mixtures are presented with discussion.

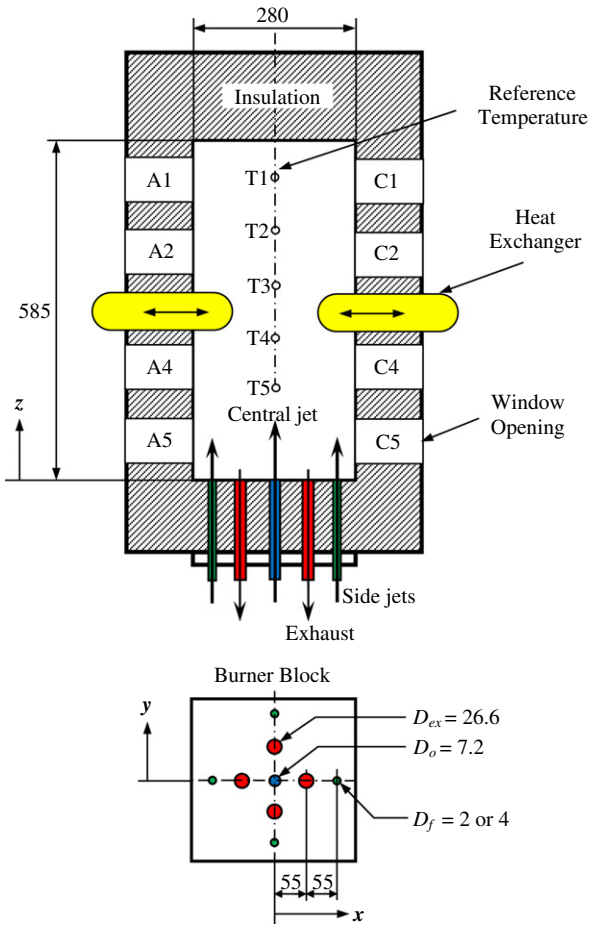

Fig. 1. Schematic figure of the MILD combustion furnace (mm in unit).

2. Experimental details

The present study uses a laboratory-scale MILD combustion furnace (MCF), shown in Fig. 1. The detail of the furnace at the University of Adelaide has been given elsewhere [42–45] and only a brief description is provided here. The combustion chamber is well insulated with four layers of 38 mm thick high-temperature ceramic fibre boards, which allows only about 20% of the total heat input to be conducted through the walls. This assists with the establishment and stability of the MILD regime, and results in a warm-up time of about 1.5 h from a cold state to steady-state operation. The MCF has five openings which are equally spaced vertically down three sides of the furnace as shown in Fig. 1. These openings can accommodate interchangeable insulating window plugs or UV grade fused silica windows. Two U-shaped cooling tubes with variable heat exchange areas are used to control the heat load. The heat exchangers can be inserted through any of the window openings, but for this investigation they are positioned in windows A3 and C3 and their exposed surface areas are 0.03 m^2 each. These heat exchangers remove 4.01 kW, 4.46 kW and 4.93 kW of heat on average for the firing rates of P = 7.5 kW, 10 kW and 15 kW, respectively.

The time-averaged furnace reference temperature (T_{ref}) is measured with a bare, fine-wire type R (Pt–Pt–13%Rh) thermocouple of 254 μm diameter wire and 1.2 mm bead diameter at steady-state conditions at the location denoted as $T1$ in Fig. 1 (x = 0, y = 0, z = 542.5 mm). This position is chosen because it is located in the post combustion zone [43] and is expected to have only products of the combustion and hence offer a reference point for all cases. The other four measurement points along the axial centerline of the furnace are also selected as temperature measurement locations $T2$–$T5$ in Fig. 1. The exhaust temperature is measured with a stainless steel sheath type K (Ni–Cr) thermocouple. Global emission levels of CO, CO_2, NO, NO_2, and O_2 are measured using a TESTO 350 XL portable gas analyzer. While uncertainties of the mean temperatures measured by thermal couples are about ±4 K, the analyzer measurement accuracies are estimated to be: [O_2] = ±0.8% of measured value, [CO] = ±10 ppm or 5% of measured value (whichever is the smallest), [NO] = ±5 ppm, [NO_2] = ±5 ppm, and [CO_2] = ±0.3% of measured value. The analyzer is checked with a calibration gas to yield total NO_x emissions accuracies better than ±5 ppm. Total NO_x emission ($NO + NO_2$) concentrations are reported by volume on a dry basis corrected to 3% O_2 concentration. By correcting to a specific O_2 level, true comparisons of emissions levels can be made because the effect of various degrees of dilutions has been removed, while still retaining a familiar mole-fraction-like variable.

The furnace is operated with a thermal input of 13 kW using three different gaseous fuels, i.e., NG, LPG, and C_2H_4. Two alternative fuel nozzles with different inner diameter are used, namely D_f = 2.0 mm and D_f = 4.0 mm. The global equivalence ratio (Φ) ranges from 0.5 to 1.4. The equivalence ratio, Φ, is defined as

$$\Phi = \frac{(O/F)_{stoic}}{(O/F)}$$

Note that the O/F is the oxidant-fuel ratio. The fuel, air, O_2 and CO_2 are introduced into the furnace at room temperature (288 K). The burner system consists of a single central tube (D_o = 7.2 mm) located on the axis of the furnace, four side fuel nozzles (D_f = 2 or 4 mm) and four exhaust ports (D_{ex} = 26.6 mm) arranged symmetrically in a ring pattern on the same wall, see Fig. 1. When NG is used as fuel, the air or O_2/CO_2 is introduced into the furnace from the central nozzle (CO_2 is premixed with the oxidant prior to its injection). When LPG or C_2H_4 is used as fuel, if the CO_2 is premixed with oxidant, the MILD combustion cannot occur no matter how much CO_2 is in use for the dilution of oxidant. Therefore, air and O_2 are injected from the central nozzle while LPG or C_2H_4 is premixed with CO_2 from the side nozzles. Table 1 summarizes all test conditions of the present experiments.

3. Results and discussion

3.1. Effect of the external CO_2 dilution

In order to investigate the influence of the CO_2 dilution, the physical properties of CO_2, N_2, O_2, H_2O, and CH_4 at 273 K and 1 atm are displayed in Table 2. It is deduced that fuel dilution by CO_2 increases the flue gas density, volume flow rate and heat capacity but decreases the kinematic viscosity, thermal conductivity and mass diffusivity. The jet momentum rate of the flue gas is calculated as $J = \int \rho U^2 \, dA$, where ρ, U, and A denote the flue-gas density, velocity and nozzle exit area, respectively. When the fuel is diluted with more CO_2, the increased ρ and U will cause an increase of J, and thus lead to stronger internal exhaust gas recirculation. The increased jet flow rate (or jet velocity) can also increase the strain rate near the fuel nozzle. Previous investigations, e.g., [44,45], indicated that the strong recirculation and high strain play a significant role in achieving MILD combustion. Indeed, this is observed in the present experiment. Figure 2 shows flame images taken for D_f = 2 mm and using LPG as fuel at Φ = 0.92. The effect of the CO_2 mass fraction in the fuel stream on the visibility of the flame is obvious: as CO_2 is increased, the flame becomes less visible and finally invisible at $Y^f_{CO2} = 60\%$ (Y^f_{CO2} denotes the initial mass fraction of CO_2 in the fuel jet). Figure 2a–d shows well-defined

Table 1
Summary of all test conditions.

Fuel	D_o (mm)	D_f (mm)	Φ	Y^f_{CO2} (%)[a]	Y^o_{CO2} (%)[b]	J_f (kg m/s^2)[c]	J_o (kg m/s^2)[d]	Mode[e]
NG	7.2	2	0.5–1	0	0–70	0.0067	0.0114–0.5231	*M* or *F*
	26	2	1	0	0	0.0067	0.0013	*F*
	7.2	4	0.5–1	0	0–70	0.0017	0.0114–0.5231	*F*
LPG	7.2	2	0.5–1	0–92	0	0.0033–0.5673	0.0089–1.3756	*M* or *F*
	7.2	4	0.5–1	0–92	0	0.0008–0.1418	0.0089–1.3756	*F*
ETH	7.2	2	0.5–1	0–90	0	0.0049–0.3345	0.0085–0.9553	*M* or *F*
	7.2	4	0.5–1	0–90	0	0.0012–0.0836	0.0085–0.9553	*F*

[a] Y^o_{CO2} denotes the mass fraction of CO_2 in the oxidant mixture.
[b] Y^f_{CO2} represents the mass fraction of CO_2 in the fuel mixture.
[c] J_f denotes the fuel jet momentum rate.
[d] J_o represents the oxidant jet momentum rate.
[e] *M* and *F* denote the MILD combustion mode and flame mode, respectively.

Table 2
Some physical properties of CO_2, N_2, O_2, H_2O and CH_4 at 273 K and 1 atm [46].

Property	Unit	CO_2	N_2	O_2	H_2O	CH_4
Density, ρ	kg/m^3	1.98	1.25	1.43	0.83	0.72
Volumetric heat capacity, c_p	kJ/(m^3 K)	1.62	1.30	1.32	1.49	1.55
Kinematic viscosity, $\upsilon \times 10^6$	m^2/s	7.09	13.30	13.60	10.12	14.50
Thermal conductivity, $\lambda \times 10^2$	W/(m K)	1.37	2.49	2.50	1.62	3.02
Absorptivity/emissivity		>0	≈0	≈0	>0	>0
Mass diffusivity in air, $\alpha \times 10^5$	m^2/s	1.38	–	1.78	2.2	1.96

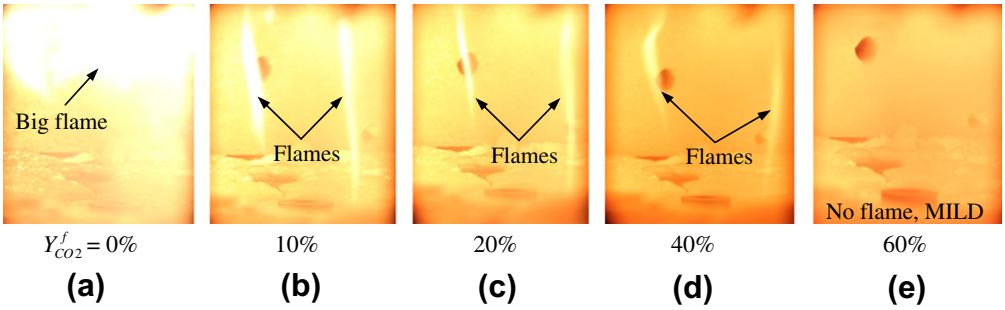

Fig. 2. Effect of CO_2 dilution on the MILD oxy-combustion of LPG with D_f = 2 mm and Φ = 0.92. Y^f_{CO2} is the mass fraction of the CO_2 in the fuel jet.

flames attached to the fuel nozzles. This suggests that the LPG/CO_2 flow strain rates are quite low and a reaction is sustained at low-oxygen and high temperature surrounding. Increasing the CO_2 fraction in the fuel stream, the flow strain rate and speed are both increased to sufficiently high values for the standard flame to 'extinguish' so that the combustion becomes invisible, i.e., MILD oxy-combustion occurs. When the MILD oxy-combustion is established (Fig. 2e), the thermal field becomes more uniform and the NO_x emission decreases from beyond 200 ppm to below 60 ppm. The MILD combustion in the present experiments is defined as the combustion where there is no visible flame front at all.

Figure 3 shows the effect of the jet momentum rate (J_o) by adding CO_2 in the oxidant stream for the NG flame at Φ = 0.95. As noted before, the temperature measurements inside the furnace use the five thermocouples *T*1 to *T*5 at *y* = 0 mm, see Fig. 1. Also given on the plot is the adiabatic flame temperature (T_{ad}), calculated from CHEMKIN with a chemical equilibrium mode, to check the temperature trend against J_o. A detailed kinetic mechanism optimized by Glarborg et al. [47] for the application in oxy-combustion is used for calculations of T_{ad} when firing CH_4 and C_2H_4 whereas that developed by Wang et al. [48] is utilized for C_3H_8.

Figure 3 demonstrates that, when the MILD combustion occurs, both the average temperature and the NO_x emission decease as the CO_2 level rises. The physical reason is noted above, i.e., the CO_2 addition increases both the jet momentum and heat capacity of the flue gas. The CO_2 increase is also expected to affect the chemistry of the NO formation. However, previous investigations [4,49–51] have suggested that the chemical effect is less significant than the physical effect. Liu et al. [49] found that the presence of CO_2 significantly reduces the local concentrations of O and H radicals, thus reducing the overall combustion rate. Park et al. [50] observed that the prompt NO and thermal NO emissions are suppressed by the recirculated CO_2 and the chemical effect. Moreover, under the fuel-lean condition, high CO_2 concentration slightly lowers NO emissions and so the chemical effect of CO_2 is not significant on NO emission [51].

For $Y^o_{CO2} = 70\%$ (Y^o_{CO2} denotes the mass fraction of CO_2 in the oxidant jet), although the in-furnace temperature is not as uniform as the cases of $Y^o_{CO2} = 53\%$ and 66% (Fig. 3), the temperature difference (<150 K) is far below that of the conventional flame. Note that the present values of T_{ad} (adiabatic flame temperature) given in Figs. 3, 4, 7 and 8 are higher than the value (≈2226 K) for the standard case of burning NG and air at constant pressure because higher oxygen fractions are taken in the present experiments. It is also worth mentioning that the CO emission level is below the detection threshold of the gas analyzer, thus not recorded.

Figure 4 reports the similar results for the cases of firing LPG (side jets) and pure oxygen (central jet). The data are obtained at

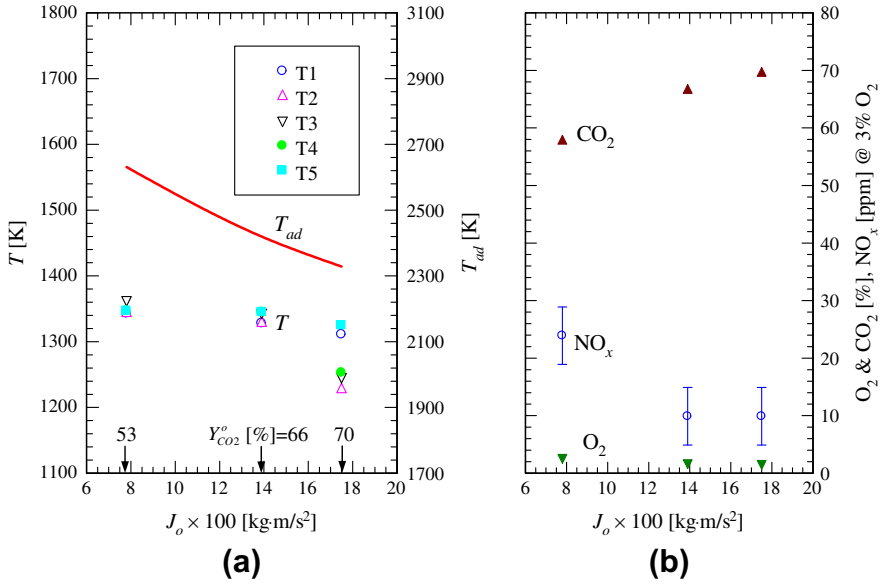

Fig. 3. Effects of the initial momentum rate of oxidant jet (J_o) on (a) the furnace temperatures and (b) exhaust emissions of NG MILD oxy-combustion at $\Phi = 0.95$. Y^o_{CO2} is the mass fraction of the CO_2 in the oxidant jet and T_{ad} is the adiabatic flame temperature.

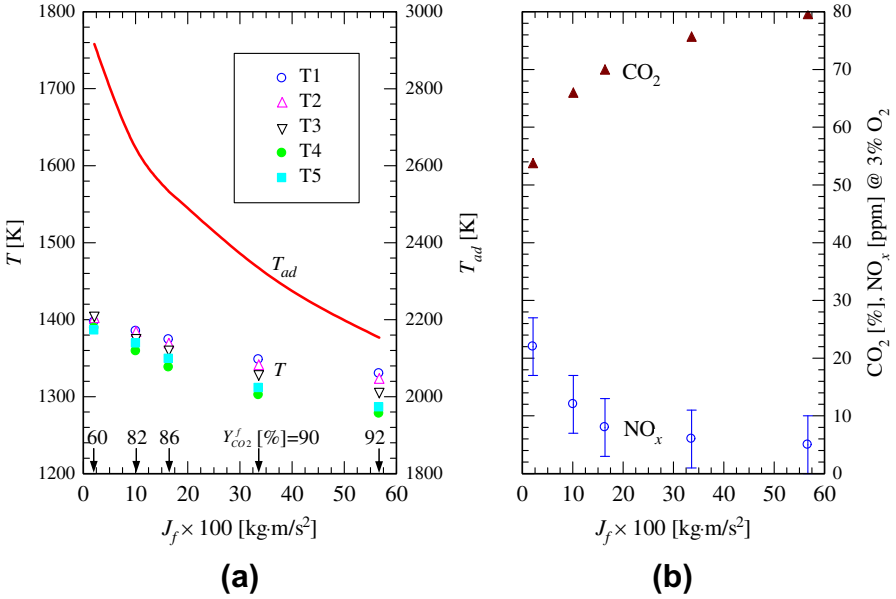

Fig. 4. Effects of the initial momentum rate of LPG/CO_2 mixture (J_f) on (a) the furnace temperature and (b) exhaust emissions of the MILD oxy-combustion at $\Phi = 1.0$. Y^f_{CO2} is the mass fraction of CO_2 in the fuel jet.

$\Phi = 1.0$ (O_2/CO_2 atmosphere) and nearly zero O_2 level in the exhaust are measured. Correspondingly, the CO_2 concentration in the flue gas is approximately 100% if the condensation of H_2O is made, so that the flue gas can be captured directly for CCS.

3.2. Effect of equivalence ratio

Figure 5a–c shows the effect of equivalence ratio (Φ) on NG oxy-combustion. Flame images are taken at $Y^o_{CO2} = 0\%$, 30% and 60% and compared. Here, the mixture of CO_2 and O_2 is discharged through the central jet nozzle. Evidently, as either Φ or Y^o_{CO2} is increased, the flame becomes less visible. It is deduced that, for a fixed value of Y^o_{CO2}, an increase in Φ leads to a transition from the standard flame to the MILD mode. One would therefore expect that, when Y^o_{CO2} is fixed, there should be a critical value of Φ, below which the MILD oxy-combustion cannot take place. Similarly, for a constant Φ, a critical value of Y^o_{CO2} should exist, below which the MILD oxy-combustion is also unable to occur. Figure 5a indicates that the MILD oxy-combustion can be achieved even when using pure oxygen ($Y^o_{CO2} = 0$) at $\Phi \approx 1.0$. Such conditions point to the effectiveness of the internal recirculation of combustion products to sustain MILD combustion with pure O_2.

The influence of equivalence ratio on the in-furnace mean temperatures and exhaust NO_x emissions is presented in Fig. 6, when firing NG and pure oxygen ($Y^o_{CO2} = 0$). The in-furnace mean temperature is obtained by averaging the temperatures measured by the five thermocouples $T1$–$T5$ (Fig. 1) at $y = 0$ mm. For $Y^o_{CO2} = 0\%$ and Φ varying from 0.5 to 0.7, there are large visible flame sheets

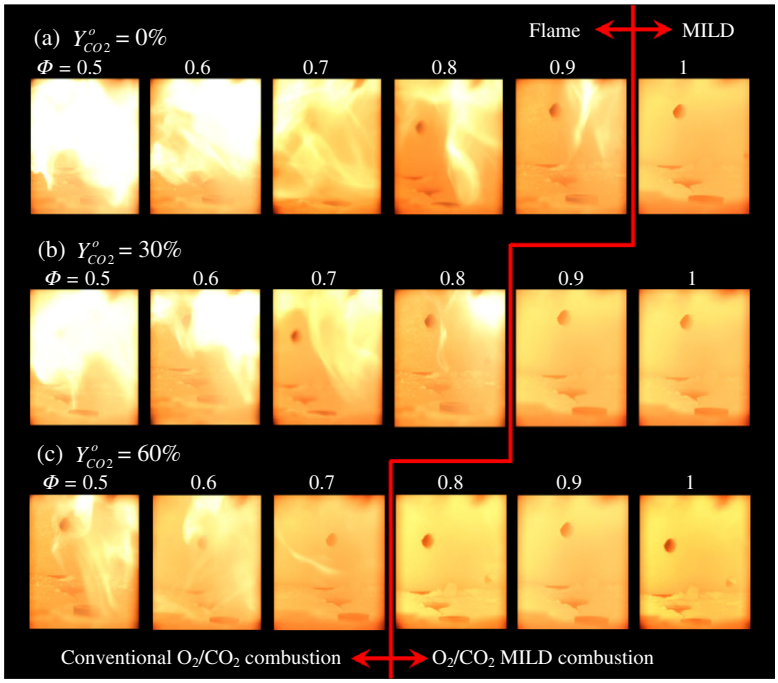

Fig. 5. Images showing the effect of equivalence ratio on the in-furnace appearance of O_2/CO_2 combustion at different initial mass fractions of CO_2 (Y^o_{CO2}) in the oxidant stream. NG is the fuel discharging from the four side nozzles while the O_2/CO_2 mixture acts as oxidant issuing through the central nozzle.

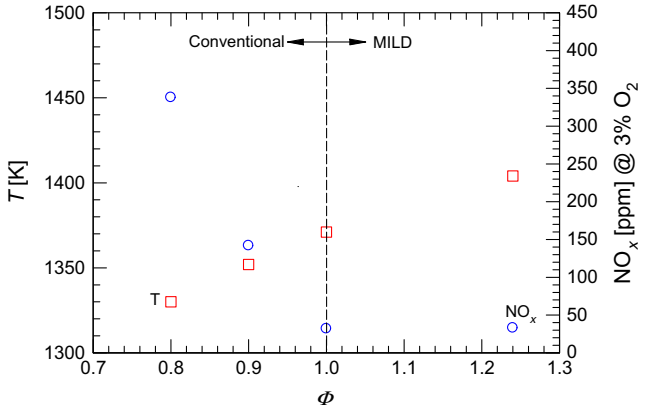

Fig. 6. Effect of equivalence ratio on the mean in-furnace temperature (T) and NO_x emissions of oxy-combustion of NG and oxygen ($Y^o_{CO2} = 0$).

in the furnace (Fig. 5a) and NO_x emissions are greater than 500 ppm (not shown on Fig. 6). When Φ is increased from 0.8 to 0.9, the flame volume decreases but the flame attached to the fuel nozzle is still clearly visible (Fig. 5a), the NO_x emissions are measured as 338 and 142 ppm, respectively. As the equivalence ratio is increased to 1.0, the flame becomes invisible (Fig. 5a) and the NO_x emission decreases to 32 ppm. The switch from the conventional oxy-fuel mode to the MILD mode occurs at $\Phi \geqslant 1.0$. Interestingly, the average temperatures at $\Phi = 0.9$ (conventional) and $\Phi = 1.0$ (MILD) are 1352 K and 1371 K, corresponding to the NO_x emissions of 142 ppm and 32 ppm, respectively. That is, the NO_x emissions decrease as the mean temperature increases due to the mode switch. In other words, higher temperatures and lower NO_x emissions are simultaneously achieved in the MILD combustion mode. This interesting result suggests that the thermal NO route should not be critical in MILD combustion. Therefore, the prompt NO and/or N_2O intermediate mechanisms are expected to be important especially at the temperature range of 1300 K to 1400 K, which will be discussed in more detail in Section 4.1.

For the MILD oxy-combustion with NG as a fuel and $\Phi \leqslant 1.0$, CO emission levels are below the detection threshold of the gas analyzer and thus they are not recorded. However, when $\Phi \approx 1.03$, although the NO_x emission is still low, very high CO emission (>500 ppm) is measured. For $\Phi = 1.24$, the combustion is still in the MILD mode and NO_x emissions are still low (Fig. 6), but the CO emission is extremely high (>3000 ppm). In this sense, the critical equivalence ratio is $\Phi_{crit} \approx 1.03$ for the non-premixed MILD oxy-combustion above which there is a steep rise in the CO emission. The critical value of Φ_{crit} was also observed in the non-premixed MILD air-combustion by Szegö et al. [42,43] and in premixed MILD air-combustion by Li et al. [44]. Interestingly, Φ_{crit} is around 0.98 and 0.90, respectively, for the premixed and non-premixed MILD air-combustions. That is, Φ_{crit} appears to be higher for the MILD oxy-combustion than for the MILD air-combustion. Such difference suggests that the high-efficiency of combustion may sustain over a wider range of Φ for the former than the latter. Note that all the above experiments used the same furnace and similar burner configuration. Szegö et al. [42,43] used $D_o = 26.6$ mm, $D_f = 2$ mm, $P = 15$ kW and NG as fuel, while Li et al. [44] burned NG at $D_o = 7.2$ mm and $P = 7.5$ and 10 kW.

Figure 7 presents the effects of equivalence ratio on the in-furnace temperature and exhaust emissions from the MILD combustion when using LPG as fuel at $Y^f_{CO2} = 60\%$. Note that the air is injected through the central nozzle, while the fuel and CO_2 are discharged through the four side nozzles. It can be seen that, as the equivalence ratio is increased significantly from $\Phi = 0.52$ to $\Phi = 0.86$, the centreline temperature increases slightly by about 10% whereas, interestingly, the NO_x emissions decrease by about 25%. Moreover, when LPG is used at $\Phi = 0.92$, the MILD oxy-combustion can be achieved by using pure oxygen, with only 30 ppm NO_x emitted. When using C_2H_4, the temperature rise due to increasing Φ is even smaller (just about 6%, Fig. 8) but the NO_x emission decreases significantly from approximately 106 ppm to 30 ppm. Therefore, there is a decrease of NO_x emissions when Φ

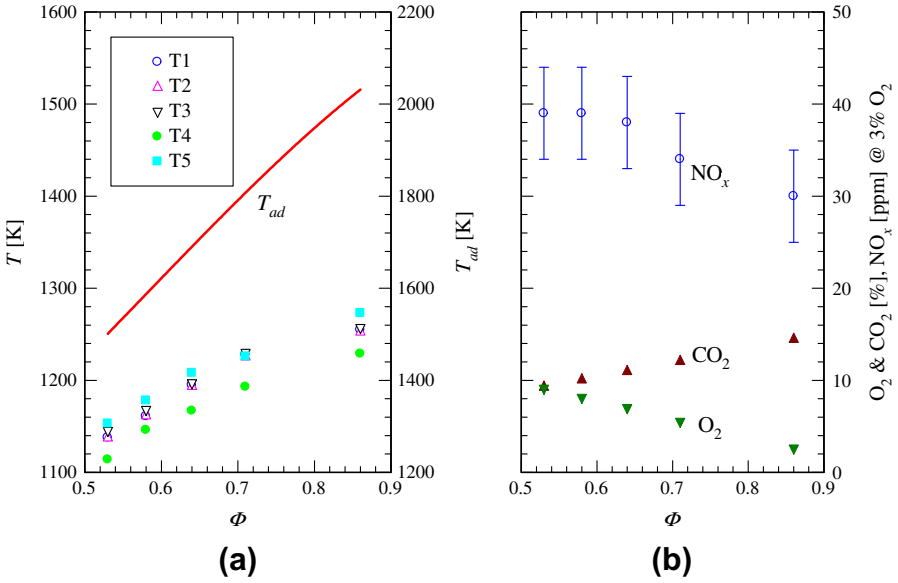

Fig. 7. Effect of equivalence ratio on (a) the temperatures and (b) exhaust emissions of MILD air-combustion by using LPG as fuel at $Y^f_{CO2} = 60\%$.

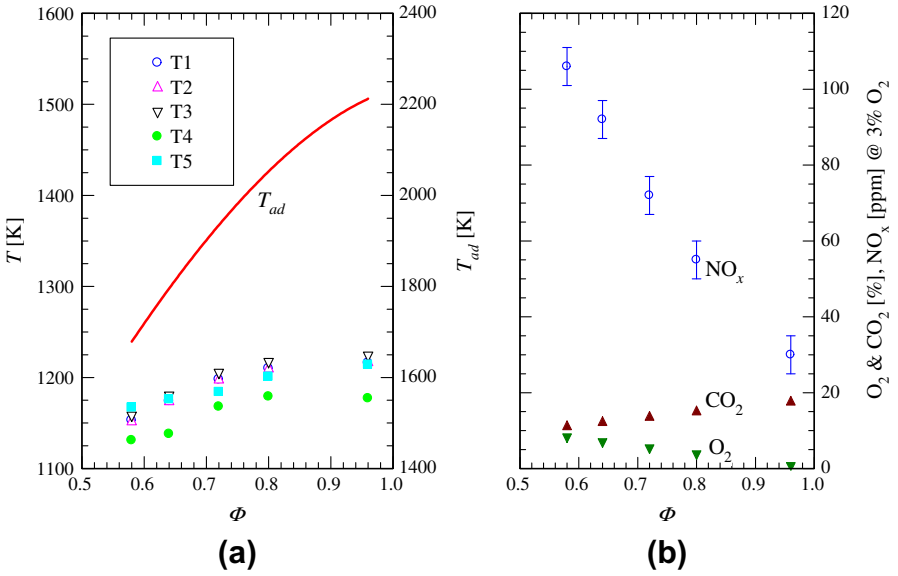

Fig. 8. Effect of equivalence ratio on (a) the temperatures and (b) exhaust emissions of MILD combustion by using C_2H_4 as fuel at $Y^f_{CO2} = 60\%$.

increases from 0.5 to 1, irrespective of the variation of fuel type, although the temperature is increased. This re-enforces the minor role that thermal NO route plays in the total NO_x emission. In other words, some other NO_x formation mechanisms may exist in the MILD combustion (see more discussions in Section 4.1).

3.3. Effect of the burner configuration

This study uses two nozzle diameters, i.e. $D_f = 4$ mm and 2 mm, for the four fuel jets. When $D_f = 4$ mm, the MILD oxy-combustion cannot be established for any fuel because of the low injection speed or momentum rate as explained in the earlier publications, e.g., [42,43]. On the other hand, for $D_f = 2$ mm, the MILD combustion occurs when firing NG. However, when changing the fuel to LPG or C_2H_4, the flame becomes visible, which is believed to derive from lower rate of the injection momentum rate (see Table 3); therefore, the establishment of their MILD combustion requires the fuel dilution with CO_2, which is described in Section 3.4.

The nozzle configurations of fuel and oxidant jets also influence the MILD oxy-combustion performance. For example, for LPG, at the thermal input of 13 kW and equivalence ratio of 0.8, the MILD combustion can be established by diluting LPG using CO_2 through

Table 3
Fuel properties of investigation.

Fuel	ρ (kg/m^3)	$h \times 10^{-4}$ (kJ/kg)	$J_f \times 10^3$ (kg m/s^2)
CH_4	0.77	4.65	6.70
LPG	2.01	4.64	3.33
C_2H_4	1.26	4.72	4.86

the side nozzles, while it cannot be achieved when premixing CO_2 and O_2 in the central jet nozzle. This can be explained. In combustor systems, the momentum rate of fuel jet is usually weaker than that of oxidant jet, which is usually termed as the 'weak jet' and 'strong jet' problem [52]. In this situation, raising the 'strong oxidant jet' momentum rate by adding CO_2 plays a minor role in changing the strain rate of the fuel jet. However, increasing the 'weak fuel jet' momentum rate is significantly different, increasing the jet strain rate, and finally extinguish the flame front attaching to the fuel nozzle and thus establish MILD combustion (Fig. 2). Therefore, in the present parallel jet burner system, the fuel jet momentum rate plays a more important role in establishing MILD combustion than that of the oxidant jet. In addition, the increased strain rate near the fuel nozzle also strengthens the small scale mixing of reactants [53], and thus suppresses soot production [37].

Moreover, the diameter of the central oxidant nozzle (D_o) influences, although much less relative to the fuel jet, the stability of the MILD oxy-combustion. For the present parallel burner configuration, the MILD oxy-combustion ($Y^o_{O2} = 100\%$) can be achieved at $\Phi \approx 1.0$, $P = 13$ kW and $D_o = 7.2$ mm. When changing D_o from 7.2 mm to 26 mm, MILD oxy-combustion cannot be reached. However, when using air instead of pure oxygen as oxidant, the MILD combustion can be established at $D_o = 26$ mm. The decrease of D_o raises the oxidant jet momentum and then enhances the recirculation of internal exhaust gas, thus enhancing the internal dilution process. It follows that, when increasing the initial oxygen level, the higher oxidant jet momentum and the stronger exhaust gas recirculation are required for the MILD combustion, which is further discussed in Sections 3.6 and 4.2.

3.4. Effect of fuel type

Our experiments demonstrate that, for the same equivalence ratio and CO_2 dilution level, the combustion mode can be different if various fuels are used. For example, when firing NG at $D_f = 2$ mm, the MILD combustion is achieved without any dilution. However, when LPG or C_2H_4 is used with $D_f = 2$ mm, if the fuel is not premixed with enough CO_2, the MILD combustion cannot occur, even with quite a large amount of CO_2 to dilute the central oxygen jet.

The effect of changing fuel on the occurrence of MILD combustion may result from different fuel injection momentum rates. To explain this, Table 3 shows the density (ρ), lower heating value (h) of each fuel considered and the injection momentum rate (J_f) without dilution. Obviously, the three fuels share nearly the same value of h. For the present investigation, when all the fuels are burnt at $P = 13$ kW, their mass flow rate (M_f) is nearly identical, i.e. $M_f = P/h \approx 2.8 \times 10^{-4}$ kg/s. Therefore, the different fuel injection momentum rates result nearly solely from their different densities because

$$J_f = M_f U = M_f \frac{M_f}{\rho A} = \left(\frac{P^2}{h^2 A}\right)\rho^{-1} = C\rho^{-1}$$

where C is approximately constant.

As shown in Table 3, the momentum rate of NG is greatly higher than those of LPG and C_2H_4. This agrees with the above observation and the effect of J_f observed in Section 3.1: i.e., the MILD mode occurs with NG but not with LPG and C_2H_4. It is also interesting that the MILD combustion of burning LPG cannot occur when diluting fuel by CO_2 even at $Y^f_{CO2} = 20\%$ but occurs at $Y^f_{CO2} = 27\%$, see Fig. 2. Note that $J_f \approx 5.22 \times 10^3$ kg m/s^2 for $Y^f_{CO2} = 20\%$ while $J_f \approx 6.28 \times 10^3$ kg m/s^2 for $Y^f_{CO2} = 27\%$. The latter momentum rate is fairly close to that ($J_f \approx 6.70 \times 10^3$ kg m/s^2) of the NG jet without dilution. Differently, however, the MILD combustion of C_2H_4 cannot take place at $Y^f_{CO2} = 25\%$ but can at $Y^f_{CO2} = 30\%$. Importantly, the momentum rates (7.85×10^3 and 8.83×10^3 kg m/s^2) in these two cases are both greater than that of NG without dilution, one by 18% and the other by 31%. Our previous work [45] has found that there is a critical value for J_f above which the MILD mode is established. In this context, it is anticipated that the critical momentum rate for burning C_2H_4 is higher than that of NG or LPG while those for the latter two are approximately identical. Such distinctions are believed to result from their different reactivities. The reactivity of C_2H_4 as an alkene member should be higher than those of CH_4 and C_3H_8 as two alkane members. Hence it is suggested that the MILD combustion achieved from burning a fuel with a higher reactivity should require a higher injection momentum rate (thus a higher critical value).

3.5. Effect of furnace temperature on NO_x emissions

Figure 9 shows the relationship between the NO_x emission and the furnace reference temperature (T_{ref}, obtained at $T1$ in Fig. 1) under all the MILD oxy conditions, i.e., only diluted by CO_2, for NG, C_2H_4 and LPG as fuel. The origin of nitrogen is in the fuel stream with NG and LPG containing N_2, respectively, of 1.28% and 0.73% by volume. The nitrogen content of C_2H_4 is unknown but expected to be slightly less than 1.0%. Worth noting is that the furnace is slightly pressurized so that no opportunity is present for outside air to leak into the furnace. With this in mind, it is understood that, the NO_x emission for burning NG or C_2H_4 is greater than that for firing LPG, due to the lower fraction of N_2 in LPG. Since all the measured mean temperatures are lower than 1400 K, the instantaneous temperatures should not be very high due to the characteristic low fluctuations in the MILD combustion. Therefore, the thermal NO accounting for the majority of NO_x emissions under the conventional flame-visible mode [5] is suppressed under the MILD mode, and thus NO_x emissions from the MILD combustion are below 60 ppm. It appears that, for each fuel, NO_x production remains constant until the temperature reaches a certain value above which the NO_x emission increases rapidly.

3.6. Effect of oxidant on the thermal field

Figure 10a and b shows, respectively, the measured furnace temperature field of the MILD air-combustion in the yz-plane ($Y^o_{O2} = 23.2\%$) and that of the MILD oxy-combustion ($Y^o_{O2} = 55.3\%$) at $\Phi = 0.82$ with NG as the fuel. Also displayed on the diagrams are schematically simplified reactant jets inside the furnace, like that given in Ref. [54]. It is shown that the 'strong' central

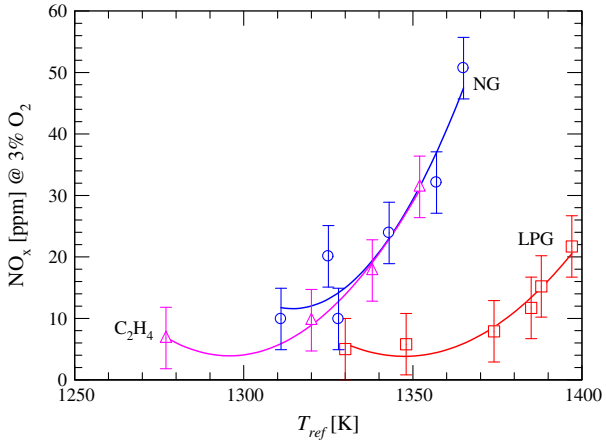

Fig. 9. Relationship between the furnace reference temperature (T_{ref}, obtained at $T1$ in Fig. 1) and NO_x emission of MILD oxy-combustion with NG, C_2H_4 or LPG as fuel.

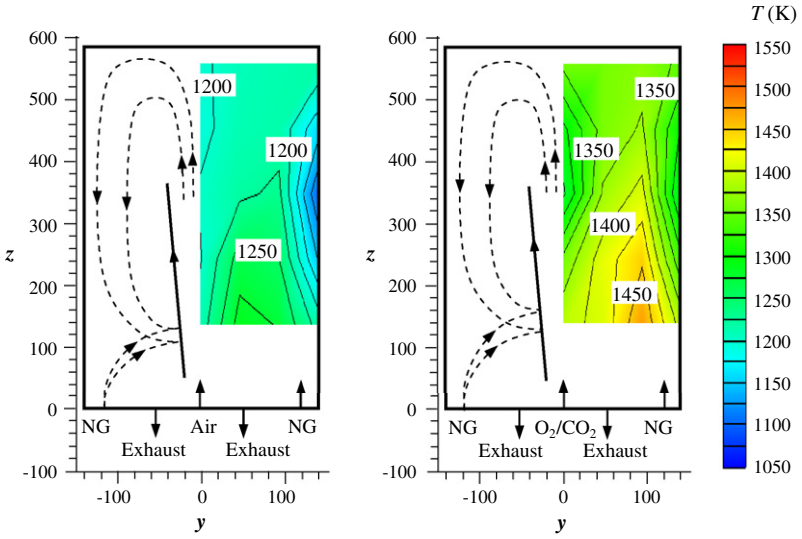

(a) MILD air-combustion (b) MILD oxy-combustion

Fig. 10. The measured furnace temperature (T) distribution in the yz-plane at $x = 0$, accompanied with a simplified diagram of the flow field derived from [54]. (a) $Y^{o}_{O2} = 23.2\%$ (O_2/N_2 environment) and (b) $Y^{o}_{O2} = 55.3\%$ (O_2/CO_2 environment). NG is fired at $\Phi = 0.82$ for both cases.

oxidant jet entrains surrounding gases and sucks the 'weak' side fuel jets, merging the latter downstream.

For both cases, the high temperature region is located in the lower part of the furnace. For the MILD air-combustion (Fig. 10a), the temperature is in the range of 1100–1300 K, compared with 1300–1450 K for the oxy-combustion (Fig. 10b). Moreover, for both cases, the thermal field is quite uniform as expected from a distributed reaction in MILD combustion. The nearly uniform thermal distribution of the MILD combustion is the result of strong flue gas recirculation inside the furnace. For the MILD air-combustion, the main operation principle has been well known and lies in the concept of exhaust gas and heat recirculation. The recirculated heat from the exhaust gas is used to raise the temperature of the reactant stream whereas the recirculated mass of the exhaust gas dilutes reactants and lowers the temperature in the reaction zone. This mechanism still holds for the MILD oxy-combustion. The increased internal recirculation enhances the convective heat transfer process [4].

However, the average temperature of the MILD oxy-combustion is higher than the MILD air-combustion by ~200 K. The reason behind this relates to the inert component of the oxidant stream. For the former, the total mass flux of the oxidant (CO_2/O_2, 6.557 kg/h) is less than that of the latter (18.870 kg/h), and thus the exhaust gas of the former is hotter at the same thermal input (13 kW).

The other difference between the two cases is that the temperature difference (ΔT) between the furnace wall (T_w) and the maximum temperatures (T_{max}) is lower for the MILD oxy-combustion. For the oxy-combustion, $\Delta T \approx 1450\ \text{K} - 1300\ \text{K} = 150\ \text{K}$ (see Fig. 10b) while, for the MILD air-combustion with, $\Delta T \approx 1300\ \text{K} - 1100\ \text{K} = 200\ \text{K}$ (see Fig. 10a). This is due to the influence of CO_2 on the radiative heat transfer. Unlike N_2 as a symmetric diatomic gas, CO_2, a triatomic gas, is not transparent to radiation. Its partial pressure in the flue gas is significantly higher in the oxy-combustion than that in the air-combustion, and hence the absorptivity and emissivity of the flue gas substantially increases, resulting in ΔT being lower.

In addition, for the MILD air-combustion, the CO_2 level in the exhaust gas is 8.2 vol% and 9.6 vol%, respectively, before and after the condensation process. The CO_2 level is low due to the addition of N_2. While for the case of MILD oxy-combustion in O_2/CO_2 environment, the CO_2 level in the flue gas is 28.6 vol% and 71.4 vol%, respectively, before and after the condensation of H_2O. The CO_2 level can be further increased to greater than 95% through externally recycling the flue gas which makes MILD oxy-combustion more suitable for CCS.

4. Further discussion

4.1. The NO_x formation mechanisms

Generally, in conventional flames, NO_x emission is mainly formed via the thermal NO route, the NO_x emission increases as the flame temperature increases. However, the present experiments reveal that, as Φ is increased, the furnace temperature (T) increases, but the NO_x emission decreases unexpectedly, regardless of the fuel type. This trend was also observed in the MILD air-combustion using the same furnace as the present study by Szegö et al. [43], although they did not discuss this point in detail. Therefore, there is a decrease in NO_x emission when increasing Φ and thus T, no matter which fuel is used whether it is in the MILD air- or oxy-combustion.

In order to better understand the mechanisms responsible for the NO_x emission in this combustion regime, the thermal-NO, prompt-NO, N_2O-intermediate, NNH and NO-reburning mechanisms are considered in the present investigation. The NO production by the oxidation of NNH radicals was proposed by Bozzelli and Dean [55]. They found that significant amounts of NO can be produced in combustion from N_2 via NNH

$$N_2 + H = NNH$$

The NNH radicals are oxidized in the subsequent reaction with O atoms

$$NNH + O = NH + NO$$

The importance of NNH mechanism has been investigated through a number of experimental and modeling studies [56–63] in premixed and non-premixed flames of both hydrogen [58–60,63] and hydrocarbon [56,57,60]. Especially, Galletti et al. [57] recently found that the NNH intermediate route must be taken into account in the MILD combustion of hydrogen containing fuels,

and Parente et al. [64] developed a simplified approach for predicting NO formation in the MILD combustion of CH_4 and H_2 blending fuels. Unlike the simplified theoretical approaches based on the perfectly stirred reactor modeling, our investigation relies on the computational fluid dynamic (CFD) simulation (using the FLUENT code [65]) considering both the actual 3-D configuration of the present furnace and detailed chemical kinematic mechanisms of the fuels. The modeling detail and validation can be found in [44,45,54] and only a brief description is provided below.

The standard k–ε model with the standard wall function is taken for modeling the turbulent flow. The eddy dissipation concept (EDC) is used for C_2H_4 and C_3H_8 with the detailed reaction mechanism of Glarborg et al. [47] and that of Prince et al. [66], respectively. Once the flow and thermal fields have been obtained from CFD and validated with the experiment, the NO route paths are calculated based on the thermal and species fields of the CFD results. The instantaneous approach is used to determine the O radical concentration in modeling NO formations from the thermal NO and N_2O-intermediate routes, as well as the OH radical concentration in thermal NO [65]. The prompt NO formation is modeled following De Soete [67]. The N_2O-intermediate mechanism is assumed at the quasi-steady-state [65]. The thermal, prompt and N_2O-intermediate routes are based on kinetic mechanisms with Arrhenius equations integrated over a probability density function (PDF) for temperature in order to take into account the effect of turbulent fluctuations on the mean reaction rates. For the NNH route, because there is no commercial code available, we use the EDC model with the NNH mechanism [61] to simulate its production (Table 4).

Figure 11 shows the calculated NO emission versus equivalence ratio (Φ) from MILD combustion for two fuels C_3H_8 and C_2H_4, under the same conditions as for those measurements shown in Figs. 7 and 8. The figure also shows the contributions of various NO mechanisms to the total NO emission. In this figure, triangle symbols denote the total NO emission considering all the NO routes (i.e., thermal, prompt, N_2O-intermediate, NNH, and NO-reburning mechanisms), square symbols represent the NO emission from the sum of thermal, prompt, N_2O-intermediate and NNH routes, and circle symbols indicate the sum of thermal, prompt and NNH routes. Evidently, the modeling qualitatively captures the experimental trend (Figs. 7 and 8): i.e., the NO emission decreases with increasing Φ, despite the value calculated being lower. Fig. 11 also demonstrates that the sum of NO formations from the thermal, prompt and NNH routes increases as Φ is increased. This can be explained. For thermal NO, as Φ is increased, the temperature increases and thus the thermal NO emission increases, although the thermal NO production rate is extremely low in the temperature range of 1150–1300 K. For the prompt NO, the NO formation results via the reactions of CH_x (e.g., CH, CH_2 and CH_3) radicals with molecular nitrogen to form HCN, and then HCN to convert to NO through various intermediates [68], e.g.,

$$CH + N_2 \leftrightarrow HCN + N$$

$$HCN + O \leftrightarrow NCO + H$$

$$NCO + H \leftrightarrow NH + CO$$

$$NH + H \leftrightarrow N + H_2$$

$$N + OH \leftrightarrow NO + H$$

Note that the first reaction is rate limiting step. Generally, as Φ is increased, the CH_x radical is increased and thus the prompt NO is increased. For the NNH route, the NNH intermediate is converted to NO through the reactions [56]

$$N_2 + H\ (+M) \leftrightarrow NNH\ (+M)$$

$$NNH + O \leftrightarrow NO + NH$$

The NNH route becomes important in fuel rich condition where the concentration of H radicals is higher [60]. Therefore, the individual increasing trends of the thermal, prompt and NNH routes with Φ indicate the trend of their sum. However, the individual contributions of the thermal, prompt and NNH NO mechanisms to the total NO emissions are not prevailing under the conditions investigated presently. The sum of the contributions from the three routes only accounts for 5–25% for the investigation cases. Moreover, a careful inspection to Fig. 11 suggests that the NO emission is mainly formed from the N_2O-intermediate route. For the intermediate N_2O mechanism, N_2 is converted to N_2O and then NO [56] via

$$N_2 + O\ (+M) \leftrightarrow N_2O\ (+M)$$

$$O + N_2O \leftrightarrow N_2 + O_2$$

$$O + N_2O \leftrightarrow NO + NO$$

At the lower temperature and oxygen-rich conditions, the intermediate N_2O route is more important. Hence, as Φ is increased, the oxygen concentration decreases and thus the N_2O-intermediate emission decreases. It is also deduced from Fig. 11 that, the NO-reburning mechanism cannot be ignored, which reduces NO emission by up to 35%. The NO-reburning mechanism denotes a group of reactions occurring in which NO is reduced by hydrocarbon radicals (CH_i) [69]. The reduction of NO by reburning is influenced by fuel mixing, temperature, stoichiometry, and gas residence time [70,71]. Giménez-López et al. [72] found that higher NO reburning efficiencies occur at moderately-high temperature (1200–1400 K), fuel-rich zone (although $\Phi < 1$), high reburn fuel concentrations, low NO initial concentrations and low H_2O concentrations. Mendiara and Glarborg [69] found that under stoichiometric and fuel-lean conditions, the NO reduction obtained in O_2/CO_2 is higher than in O_2/N_2 atmosphere. The NO-reburning mechanism was also evidenced to occur in the MILD combustion regime [73–75]. Nicolle et al. [73] found, via chemical kinetic modeling, that the NO-reburning reactions are particularly active in the fuel-ignition chemistry and the NO reduction increases as Φ is increased from 0.5 to 1.5. The experimental evidence was also observed in MILD combustion by Mancini et al. [33] using NG as fuel and Schaffel et al. [74] under the pulverized coal combustion. Mancini et al. [33] found, through measurement and reactor network modeling, that there was no formation of NO within the fuel jet, where the exhaust gas was recirculated into and the NO was reduced due to the fuel-rich there. From experiment and CFD modeling, Schaffel et al. [74] found a strong NO-reburning existing downstream from the position where the fuel and air jets are merged. They believed that less NO was formed from combustion of volatiles and stronger NO-reburning mechanisms in the MILD combustion compared to the conventional combustion. Therefore, the NO-reburning mechanism is expected to occur in the fuel-rich zone and thus reduces the global NO emission of MILD combustion.

Table 4
Chemical reactions in the NHH mechanism for the NO formation[a] [61].

		A	n	E
1	$NNH = N_2 + H$	1.0×109	0.000	0
2	$NNH + O = NH + NO$	5.2×10^{11}	0.388	−409
3	$NH + O = NO + H$	9.2×10^{13}	0.000	0
4	$NH + O_2 = NO + OH$	1.3×10^{6}	1.500	100

[a] The reaction rate coefficient $k = A\,T^n \exp(-E/RT)$, where R is the universal gas constant and T is the temperature. Units are cm, mol, s, cal.

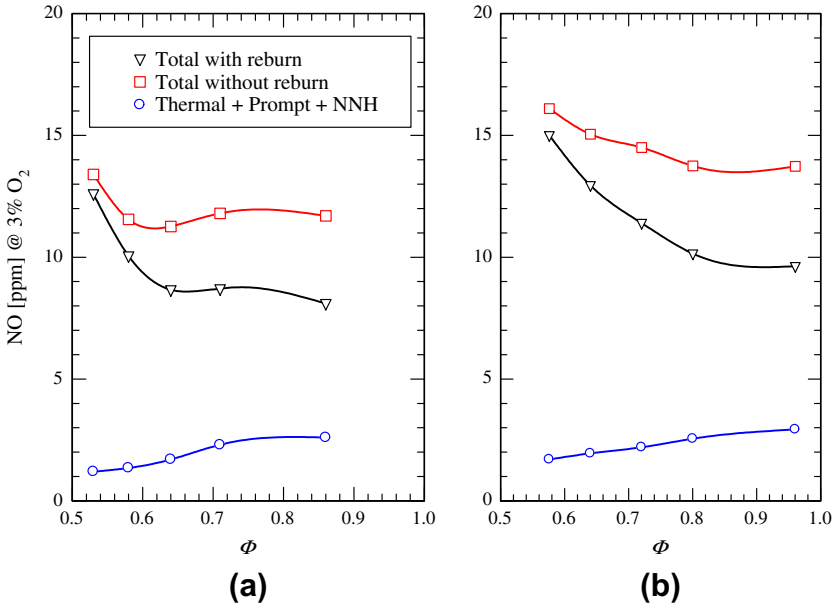

Fig. 11. Calculated NO emission versus equivalence ratio (Φ) from MILD combustions of (a) C_3H_8 and (b) C_2H_4, under the same conditions as for the measured data in Figs. 7 and 8.

4.2. Stability limits

Wünning and Wünning [20] reported on the stability limits of the MILD combustion for methane and air. They classified three combustion regimes (stable flames, unstable flame and MILD combustion) based on the furnace temperature (T) and the relative recirculation rate K_v defined by

$$K_v = M_d/(M_o + M_f)$$

Here, M_d and ($M_o + M_f$) denote the total mass fluxes of diluents and the injecting reactants (i.e., the oxidant and the fuel), respectively; $M_d = M_i + M_e$, where M_i and M_e are the mass flow rates of the *internal* entrained exhaust gas and the *external* diluents. In general, it is extremely difficult to measure K_v by experiment. Thus, for the present furnace system, the estimate of K_v is obtained using the CFD simulation [75,76]. Nevertheless, if the combustor is specially designed like, e.g., those in Refs. [20,57,77], K_v may be obtained by the direct measurements of M_d.

Wünning and Wünning [20] defined the flameless oxidation (FLOX) or MILD combustion regimes based on $K_v > 3$ and $T > 1100$ K when using methane as fuel and air as oxidant. The present study has found that, as the initial oxygen fraction (Y^o_{O2}) increases, more recirculated exhaust gas is needed for the MILD combustion to occur. Accordingly, the stability of the MILD combustion is controlled also by Y^o_{O2}. Considering this, the diagram of the stability limits of the MILD combustion from Wünning and Wünning [20] is modified to a diagram in the $K_v - T - Y^o_{O2}$ space for N_2 to be the diluent, as illustrated in Fig. 12. The stability boundary of the MILD air-combustion at $Y^o_{O2} = 23.2\%$ (green[1] lines) is obtained from the data of Wünning and Wünning [20].

When Y^o_{O2} is increased, the limit of K_v should be increased as reasoned below. In the present experiments, for example, the MILD air-combustion ($Y^o_{O2} = 23.2\%$) occurs when the diameter of the central nozzle is taken to be D_o = 26 mm, while the MILD oxy-combustion cannot take place at D_o = 26 mm, but occurs at D_o = 7.2 mm for $Y^o_{O2} = 50\%$; the decrease in D_o increases the initial jet momentum rate of the mixture (J_o) by about 13 times from 8.38×10^{-3} kg m/s^2 to 10.93×10^{-2} kg m/s^2, noting that $J_o = \int \rho_o U_o^2 \, dA = \int_0^{D_o/2} \rho_o U_o^2 \cdot 2\pi r dr = 4m_o^2/(\rho_o \pi D_o^2)$, where m_o denotes the jet mass flow rate which is kept constant in the experiment. Such a great increase in J_o dramatically boosts the internal recirculation and thus increases K_v. Therefore, as Y^o_{O2} is increased, K_v has to be increased in order to establish the MILD condition and hence the oxy-enriched MILD combustion region is reduced in size (Fig. 12, red lines). When reactants are diluted externally by N_2 to achieve $Y^o_{O2} = 6\%$ before they enter the furnace, even relatively-weak internal recirculation or dilution can make MILD combustion to occur and thus the oxy-diluted MILD region is expanded (blue lines). The stability limits for the oxy-diluted MILD combustion at $Y^o_{O2} < 23.2\%$, MILD air-combustion at $Y^o_{O2} = 23.2\%$ and oxy-enriched MILD combustion at $Y^o_{O2} > 23.2\%$ are delimited by the shadow surface and displayed in the $K_v - T - Y^o_{O2}$ space of Fig. 12. Note that K_v represents both the *internal and external* dilutions by recirculated exhaust gases whereas Y^o_{O2} denotes the low-oxygen fraction after *external* dilution by diluents such as N_2, CO_2 or recycled exhaust gases.

Furthermore, as demonstrated in Section 3.2, the MILD combustion occurs only when sufficiently high is the equivalence ratio (Φ) or the *external* relative dilution rate K^*_v [$=M_e/(M_o + M_f)$, where M_e is the mass flow rate of the externally recirculated exhaust gas or other initial diluents]. Chen et al. [4] proposed schematically a flammable region diluted by N_2 or CO_2 in the $K^*_v - \Phi - T_p$ space, which is reproduced in Fig. 13 (T_p denotes the preheat temperature of the oxidant). This flammable region is extended to a higher value of K^*_v when reactants are preheated and when Φ is closer to stoichiometric. The envelope of the flammable region defines the critical operating conditions beyond which blowout occurs. Combustion becomes less stable as the operating conditions approach the flammable surface. The smaller flammable region (surrounded by red lines), when changing the dilution gas from N_2 to CO_2, is caused by the lower combustion temperature resulting from the higher molar heat capacity of CO_2, and the lower reaction rate caused by the chemical effect of CO_2 [4].

[1] For interpretation of color in Fig. 12, the reader is referred to the web version of this article.

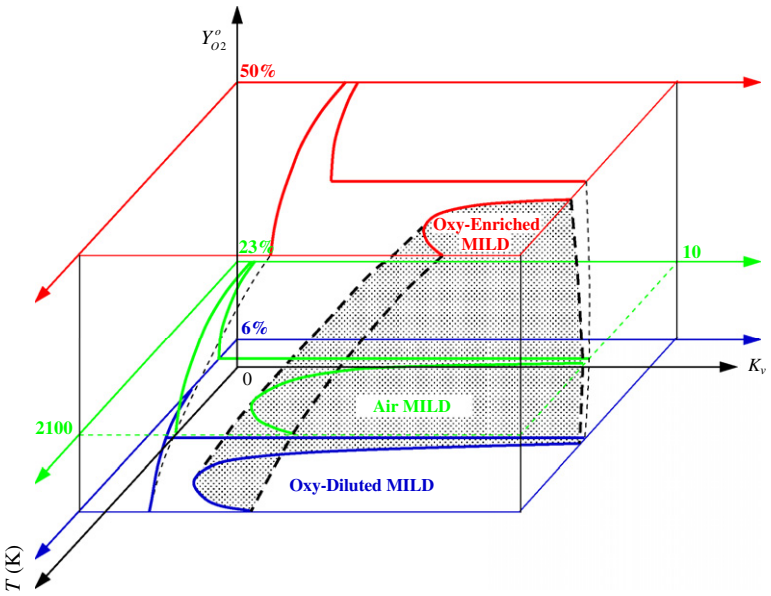

Fig. 12. Schematic diagram of the stability limits for different combustion modes in the $K_v - T - Y^o_{02}$ space. K_v, T and Y^o_{02} denote the exhaust recirculation rate, furnace temperature (K) and initial mass fraction of O_2 (%) diluted by N_2, respectively.

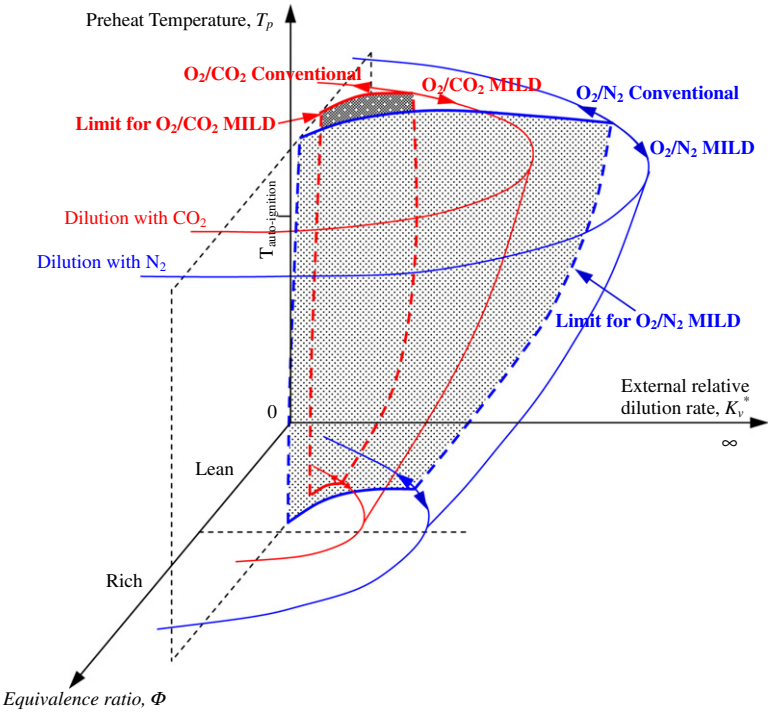

Fig. 13. Schematic diagram of the stability limits for MILD combustion in the flammable domain of $K_v^* - \Phi - T_p$ space. K_v^*, Φ and T_p denote the external relative dilution ratio, equivalence ratio and the preheat temperature of oxidant, respectively.

According to the present experiments, the MILD combustion takes place only when Φ or K_v^* is sufficiently high. For instance, when firing NG at $Y^o_{CO2} = 30\%$, the MILD combustion cannot occur when $\Phi \leqslant 0.8$ but can at $\Phi \geqslant 0.9$ (Fig. 5b). For $Y^o_{CO2} = 60\%$, the MILD combustion is not established at $\Phi \leqslant 0.7$ but occurs at $\Phi \geqslant 0.8$ (Fig. 5c). That is, for a fixed value of Y^o_{CO2}, an increase in Φ leads to a transition from the standard flame to the MILD mode; similarly, for a constant Φ, an increase in Y^o_{CO2} causes a switch from the conventional mode to MILD mode. Therefore, the stability limits of MILD combustion can be defined in the flammable domain of $K_v^* - \Phi - T_p$ space, as displayed also in Fig. 13. Interestingly, when changing the dilution gas from N_2 (blue) to CO_2 (red), the MILD region extends significantly to lower Φ and lower K_v^* region. It is thus concluded that at a fixed Φ, the O_2/CO_2 MILD combustion is easier to occur than the O_2/N_2 MILD combustion, because the less dilution is required for the former case. In addition, Fig. 13 suggests that, relative to the O_2/CO_2 case, the O_2/N_2 MILD combustion can be sustained at a larger Φ or K_v^* or both.

5. Conclusions

The present study has investigated the operational characteristics of the MILD oxy-combustion using natural gas (NG), liquefied petroleum gas (LPG) and ethylene (C_2H_4) in the combustor system shown in Fig. 1. Specifically, the influences of equivalence ratio (Φ), the diameter of the fuel nozzle, CO_2 dilutions in reactants and different fuels have been examined experimentally. It has been demonstrated that the MILD oxy-combustion can be achieved using the three fuels, even with pure oxygen as oxidant. When the MILD oxy-combustion is established, quite a uniform temperature distribution and very low emissions of NO_x and CO are obtained. The measured furnace temperatures and exhaust emissions of MILD oxy-combustion have been presented and discussed in Sections 3 and 4. To analyze the NOx emissions of MILD combustion, the CFD modeling has been taken for burning C_2H_4 and C_3H_8 (close to LPG), whose results are given in Section 4.1. The main conclusions with several new findings are summarized below:

(1) The initial fuel dilution by CO_2 significantly impacts the oxy-combustion. When the oxy-combustion is in the conventional mode at low CO_2 levels, the dilution reduces the size of visible flame and the intensity of combustion. Further dilution enhances the occurrence of MILD combustion. In the MILD region, more dilution can further lower the furnace temperature and exhaust NO_x emissions.

(2) The fuel-jet momentum rate is generally the most critical parameter for establishing the MILD oxy-combustion. In the present furnace system, both the use of a smaller diameter of the fuel nozzle and the fuel dilution by CO_2 result in a higher fuel-jet momentum rate and thus promote the occurrence of MILD combustion. Similarly, without any dilution, MILD combustion develops more easily when burning NG than using LPG and C_2H_4 due to a higher momentum of the NG jet.

(3) Higher fuel-injection momentum rates are required for burning higher-reactivity fuels for the MILD combustion. The reactivity of C_2H_4 as the alkene member is higher than those of CH_4 and C_3H_8 as the alkane members. Hence, the momentum rate for achieving MILD combustion when burning C_2H_4 is greater than those of NG and LPG.

(4) The equivalence ratio Φ has significant influence on the MILD combustion. At fixed CO_2 dilution levels, the MILD condition can be achieved only when Φ is sufficiently high. When $\Phi < 1$, as Φ is increased, the furnace temperature rises slightly but the NO_x emission decreases, no matter which fuel is burnt and which inert is used for dilution. This finding cannot be explained when using the traditional thermal NO_x mechanism.

(5) Under the present MILD conditions, by the CFD modeling, the NO emission results mainly from the intermediate N_2O route, rather than from the thermal, prompt and NNH NO mechanisms; the NO emissions from the latter three are estimated altogether to be 5–25% of the total NO emission. As Φ is increased, the NO formation from the intermediate N_2O route decreases while the NO-reburning mechanism becomes more important. It is also worth noting that the NO-reburning cannot be ignored because its presence may reduce the total NO emission by up to 35%.

(6) The stability limits for the MILD combustion mode can be illustrated by the $K_v - T - Y^o_{O2}$ and also the $K^*_v - \Phi - T_p$ diagrams (Figs. 12 and 13). A stronger flue gas recirculation is needed for establishing the oxy-enriched MILD combustion, and thus the oxy-enriched MILD combustion region is reduced in Fig. 12 relative to the air–fuel MILD combustion. In addition, when changing the diluents from N_2 to CO_2, the MILD combustion region extends significantly to lower values of Φ and lower external relative dilution rates (Fig. 13), demonstrating that the MILD O_2/CO_2 combustion is easier to occur than does the MILD O_2/N_2 combustion.

Acknowledgments

The support of both Specific Research Fund for Doctoral Program of Higher Education of China (No. 20110001130014) and Nature Science Foundation of China (No. 51276002) is gratefully acknowledged. We would also like to thank all the referees for their insightful comments and criticisms on the early version of this manuscript, the addressing of which has significantly strengthened the work.

References

[1] S. Chu, Science 325 (5948) (2009) 1599.
[2] T. Wall, Proc. Combust. Inst. 31 (1) (2007) 31–47.
[3] A.F. Ghoniem, Prog. Energy Combust. Sci. 37 (1) (2011) 15–51.
[4] L. Chen, S.Z. Yong, A.F. Ghoniem, Prog. Energy Combust. Sci. 38 (2) (2012) 156–214.
[5] F. Normann, K. Andersson, B. Leckner, F. Johnsson, Prog. Energy Combust. Sci. 35 (5) (2009) 385–397.
[6] M.B. Toftegaard, J. Brix, P.A. Jensen, P. Glarborg, A.D. Jensen, Prog. Energy Combust. Sci. 36 (5) (2010) 581–625.
[7] K. Andersson, F. Johnsson, Fuel 86 (5–6) (2007) 656–668.
[8] E. Kakaras, A. Koumanakos, A. Doukelis, D. Giannakopoulos, I. Vorrias, Fuel 86 (14) (2007) 2144–2150.
[9] R.S. Haszeldine, Science 325 (5948) (2009) 1647–1652.
[10] DOE US. Secretary Chu Announces FutureGen 2.0, <http://www.energy.gov/9309.htm> (05.08.10)
[11] B.J.P. Buhre, L.K. Elliott, C.D. Sheng, R.P. Gupta, T.F. Wall, Prog. Energy Combust. Sci. 31 (4) (2005) 283–307.
[12] T. Wall, Y. Liu, C. Spero, L. Elliott, S. Khare, R. Rathnam, F. Zeenathal, B. Moghtaderi, B. Buhre, C. Sheng, R. Gupta, T. Yamada, K. Makino, J. Yu, Chem. Eng. Res. Des. 87 (8) (2009) 1003–1016.
[13] T. Wall, J. Yu, in: The 34th International Technical Conference on Clean Coal & Fuel Systems, Clearwater, Florida, USA, 2009.
[14] T. Nozaki, S. Takano, T. Kiga, Energy 22 (2–3) (1997) 199–205.
[15] N. Kimura, K. Omata, T. Kiga, S. Takano, S. Shikisima, Energy Convers. Manage. 36 (6–9) (1995) 805–808.
[16] T. Suda, K. Masuko, J. Sato, A. Yamamoto, K. Okazaki, Fuel 86 (12–13) (2007) 2008–2015.
[17] S. Turns, An Introduction to Combustion: Concepts and Applications, McGraw-Hill, New York, 1996.
[18] A. Cavaliere, M. de Joannon, Prog. Energy Combust. Sci. 30 (4) (2004) 329–366.
[19] H. Tsuji, A.K. Gupta, T. Hasegawa, M. Katsuki, K. Kishimoto, M. Morita, High Temperature Air Combustion, CRC Press, Boca Paton, FL, 2003.
[20] J.A. Wünning, J.G. Wünning, Prog. Energy Combust. Sci. 23 (1997) 81–94.
[21] M. Katsuki, T. Hasegawa, Proc. Combust. Inst. 27 (2) (1998) 3135–3146.
[22] R. Weber, S. Orsino, N. Lallemant, A. Verlaan, Proc. Combust. Inst. 28 (1) (2000) 1315–1321.
[23] R. Weber, A. Lverlaan, S. Orsino, N. Lallemant, J. Energy Inst. 72 (1999) 77–83.
[24] T. Plessing, N. Peters, J.G. Wünning, Proc. Combust. Inst. 27 (2) (1998) 3197–3204.
[25] International Flame Research Foundation, <http://www.ifrf.net/>.
[26] M. de Joannon, A. Cavaliere, R. Donnarumma, R. Ragucci, Proc. Combust. Inst. 29 (1) (2002) 1139–1146.
[27] M. de Joannon, A. Cavaliere, T. Faravelli, E. Ranzi, P. Sabia, A. Tregrossi, Proc. Combust. Inst. 30 (2) (2005) 2605–2612.
[28] M. de Joannon, A. Matarazzo, P. Sabia, A. Cavaliere, Proc. Combust. Inst. 31 (2) (2007) 3409–3416.
[29] M. Derudi, A. Villani, R. Rota, Proc. Combust. Inst. 31 (2) (2007) 3393–3400.
[30] C. Galletti, A. Parente, L. Tognotti, Combust. Flame 151 (4) (2007) 649–664.
[31] A. Effuggi, D. Gelosa, M. Derudi, R. Rota, Combust. Sci. Technol. 180 (3) (2008) 481–493.
[32] R. Weber, J.P. Smart, W. vd Kamp, Proc. Combust. Inst. 30 (2) (2005) 2623–2629.
[33] M. Mancini, P. Schwöppe, R. Weber, S. Orsino, Combust. Flame 150 (1–2) (2007) 54–59.
[34] N. Lallemant, F. Breussin, R. Weber, T. Ekman, J. Dugue, J.M. Samaniego, O. Charon, A.J. Van Den Hoogen, J. Van Der Bemt, W. Fujisaki, T. Imanari, T. Nakamura, K. Iino, J. Energy Inst. 73 (2000) 169–182.
[35] F. Breussin, N. Lallemant, R. Weber, Combust. Sci. Technol. 160 (2000) 369–397.
[36] W. Blasiak, W.H. Yang, K. Narayanan, J. von Schéele, J. Energy Inst. 80 (1) (2007) 3–11.

[37] N. Krishnamurthy, P.J. Paul, W. Blasiak, Proc. Combust. Inst. 32 (2) (2009) 3139–3146.
[38] N. Krishnamurthy, W. Blasiak, A. Lugnet, in: Proceedings of the Joint International Conference on Sustainable Energy and Environment, Hua Hin, Thailand, 2004, vol. II, pp. 552–557.
[39] H. Stadler, D. Ristic, M. Förster, A. Schuster, R. Kneer, G. Scheffknecht, Proc. Combust. Inst. 32 (2) (2009) 3131–3138.
[40] H. Stadler, D. Christ, M. Habermehl, P. Heil, A. Kellermann, A. Ohliger, D. Toporov, R. Kneer, Fuel 90 (4) (2011) 1604–1611.
[41] P. Heil, D. Toporov, M. Förster, R. Kneer, Proc. Combust. Inst. 33 (2) (2011) 3407–3413.
[42] G.G. Szegö, B.B. Dally, G.J. Nathan, Combust. Flame 154 (1–2) (2008) 281–295.
[43] G.G. Szegö, B.B. Dally, G.J. Nathan, Combust. Flame 156 (2) (2009) 429–438.
[44] P. Li, J. Mi, B.B. Dally, R.A. Craig, F. Wang, Energy Fuel 25 (7) (2011) 2782–2793.
[45] J. Mi, P. Li, B.B. Dally, R.A. Craig, Energy Fuel 23 (11) (2009) 5349–5356.
[46] NIST Chemistry WebBook: Thermophysical Properties of Fluid Systems, 2009 <http://webbook.nist.gov/chemistry/>.
[47] P. Glarborg, L.L.B. Bentzen, Energy Fuel 22 (2008) 291–296.
[48] H. Wang, X. You, A.V. Joshi, S.G. Davis, A. Laskin, F. Egolfopoulos, C.K. Law, USC Mech Version II. High-Temperature Combustion Reaction Model of H2/CO/C1-C4 Compounds, May 2007 <http://ignis.usc.edu/USC_Mech_II.htm>.
[49] F. Liu, H. Guo, G.J. Smallwood, Combust. Flame 133 (2003) 495–497.
[50] J. Park, J.S. Park, H.P. Kim, J.S. Kim, S.C. Kim, J.G. Choi, H.C. Cho, K.W. Cho, H.S. Park, Energy Fuel 21 (2007) 121–129.
[51] R. Zhao, H. Liu, X. Zhong, Z. Wang, H. Hu, J. Qiu, Fuel Process. Technol. 92 (2011) 939–945.
[52] E.W. Grandmaison, I. Yimer, H.A. Becker, A. Sobiesiak, Combust. Flame 114 (3–4) (1998) 381–396.
[53] G.J. Nathan, J. Mi, Z.T. Alwahabi, G.J.R. Newbold, D.S. Nobes, Prog. Energy Combust. Sci. 32 (5–6) (2006) 496–538.
[54] J. Mi, F. Wang, P. Li, B.B. Dally, Energy Fuel 26 (2012) 265–277.
[55] J.W. Bozzelli, A.M. Dean, Int. J. Chem. Kin. 27 (1995) 1097–1110.
[56] J. Tomeczek, B. Gradon, Combust. Flame 133 (2003) 311–322.
[57] C. Galletti, A. Parente, M. Derudi, R. Rota, L. Tognotti, Int. J. Hydrogen Energy 34 (19) (2009) 8339–8351.
[58] A.A. Konnov, G. Colson, J. de Ruyck, Combust. Flame 121 (2000) 548–550.
[59] M. Skottene, K.E. Rian, Int. J. Hydrogen Energy 32 (15) (2007) 3572–3585.
[60] A.N. Hayhurst, E.M. Hutchinson, Combust. Flame 114 (1998) 274–279.
[61] S.J. Klippenstein, L.B. Harding, P. Glarborg, J.A. Miller, Combust. Flame 158 (4) (2011) 774–789.
[62] D. Charlston-goch, B.L. Chadwick, R.J.S. Morrison, A. Campisi, D.D. Thomsen, N.M. Laurendeau, Combust. Flame 125 (2001) 729–743.
[63] G.J. Rørtveit, J.E. Hustad, S.C. Li, F.A. Williams, Combust. Flame 130 (2002) 48–61.
[64] A. Parente, C. Galletti, L. Tognotti, Proc. Combust. Inst. 33 (2) (2011) 3343–3350.
[65] Fluent 6.3 Documentation. Fluent Inc., 2007.
[66] J.C. Prince, F.A. Williams, Combust. Flame 159 (2012) 2336–2344.
[67] G.G. De Soete, Proc. Combust. Inst. 15 (1) (1975) 1093–1102.
[68] C.T. Bowman, Proc. Combust. Inst. 24 (1) (1992) 859–878.
[69] T. Mendiara, P. Glarborg, Energy Fuel 23 (2009) 3565–3572.
[70] D. Kühnemuth, F. Normann, K. Andersson, F. Johnsson, B. Leckner, Energy Fuel 25 (2011) 624–631.
[71] F. Normann, K. Andersson, F. Johnsson, B. Leckner, Ind. Eng. Chem. Res. 49 (2010) 9088–9094.
[72] J. Giménez-López, V. Aranda, A. Millera, R. Bilbao, M.U. Alzueta, Fuel Process. Technol. 92 (2011) 582–589.
[73] A. Nicolle, P. Dagaut, Fuel 85 (2006) 2469–2478.
[74] N. Schaffel, M. Mancini, A. Szlęk, R. Weber, Combust. Flame 156 (9) (2009) 1771–1784.
[75] P. Li, J. Mi, Flow Turbul. Combust. 87 (4) (2011) 1–22.
[76] J. Mi, P. Li, C. Zheng, Energy 36 (11) (2011) 6583–6595.
[77] A. Parente, C. Galletti, L. Tognotti, Int. J. Hydrogen Energy 33 (24) (2008) 7553–7564.